Accepted Manuscript

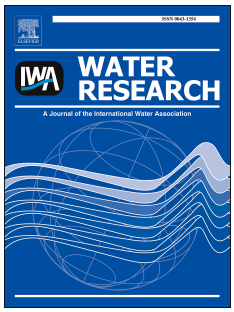

Kinetics and mechanisms of nitrate and ammonium formation during ozonation of dissolved organic nitrogen

Glen Andrew D. de Vera, Wolfgang Gernjak, Howard Weinberg, Maria José Farré, Jurg Keller, Urs von Gunten

PII: S0043-1354(16)30771-0

DOI: 10.1016/j.watres.2016.10.021

Reference: WR 12419

To appear in: *Water Research*

Received Date: 27 July 2016

Revised Date: 4 October 2016

Accepted Date: 7 October 2016

Please cite this article as: de Vera, G.A.D., Gernjak, W., Weinberg, H., Farré, M.J., Keller, J., von Gunten, U., Kinetics and mechanisms of nitrate and ammonium formation during ozonation of dissolved organic nitrogen, *Water Research* (2016), doi: 10.1016/j.watres.2016.10.021.

Kinetics and mechanisms of nitrate and ammonium formation during ozonation of dissolved organic nitrogen

Glen Andrew D. de Vera[1,5], Wolfgang Gernjak[1,2,3], Howard Weinberg[4], Maria José Farré[1,2], Jurg Keller[1*], Urs von Gunten[5,6*]

[1]The University of Queensland (UQ), Advanced Water Management Centre, Queensland 4072, Australia

[2]ICRA, Catalan Institute for Water Research, Scientific and Technological Park of the University of Girona, H_2O Building, Emili Grahit 101, 17003 Girona, Spain

[3]ICREA, Catalan Institute for Research and Advanced Studies, 08010 Barcelona, Spain

[4]University of North Carolina at Chapel Hill, Department of Environmental Sciences and Engineering, 146A Rosenau Hall, Chapel Hill, North Carolina 27599, United States

[5]School of Architecture, Civil and Environmental Engineering (ENAC), École Polytechnique Fédérale de Lausanne (EPFL), CH-1015, Lausanne, Switzerland

[6]Eawag, Swiss Federal Institute of Aquatic Science and Technology, Ueberlandstrasse 133, CH-8600 Duebendorf, Switzerland

[*]Corresponding authors:

Jurg Keller: Phone: +61733654727; fax: +61733654726; email: j.keller@uq.edu.au

Urs von Gunten: Phone: +41587655270; fax: +41587655210; email: vongunten@eawag.ch

Submitted to Water Research

Abstract

Dissolved organic nitrogen (DON) is an emerging concern in oxidative water treatment because it exerts oxidant demand and may form nitrogenous oxidation/disinfection by-products. In this study, we investigated the reactions of ozone with DON with a special emphasis on the formation of nitrate (NO_3^-) and ammonium (NH_4^+). In batch ozonation experiments, the formation of NO_3^- and NH_4^+ was investigated for natural organic matter standards, surface water, and wastewater effluent samples. A good correlation was found between NO_3^- formation and the O_3 exposure ($R^2 > 0.82$) during ozonation of both model DON solutions and real water samples. To determine the main precursor of NO_3^-, solutions composed of tannic acid and model compounds with amine functional groups were ozonated. The NO_3^- yield during ozonation was significantly higher for glycine than for trimethylamine and dimethylamine. Experiments with glycine also showed that NO_3^- was formed via an intermediate with a second-order rate constant of 7.7 ± 0.1 $M^{-1}s^{-1}$ while NH_4^+ was formed by an electron-transfer mechanism with O_3 as confirmed from a hydroxyl radical ($^{\bullet}OH$) yield of 24.7 ± 1.9%. The NH_4^+ concentrations, however, were lower than the $^{\bullet}OH$ yield (0.03 mol NH_4^+/mol $^{\bullet}OH$) suggesting other $^{\bullet}OH$-producing reactions that compete with NH_4^+ formation. This study concludes that NO_3^- formation during ozonation of DON is induced by an oxygen-transfer to nitrogen forming hydroxylamine and oxime, while NH_4^+ formation is induced by electron-transfer reactions involving C-centered radicals and imine intermediates.

Keywords: ozonation, dissolved organic nitrogen, O_3 exposure, nitrate, ammonium

1. Introduction

Dissolved organic nitrogen (DON) in the aquatic environment commonly occurs as amino acids, peptides and proteins and accounts for 0.5 – 10% (by mass) of the dissolved organic matter (DOM) (Sharma and Graham 2010, Westerhoff and Mash 2002). Despite these relatively low concentrations, DON is considered an emerging concern for water utilities because it can act as precursor of potentially toxic nitrogenous oxidation/disinfection by-products (e.g., nitrosamines, halonitromethanes, haloacetonitriles) during chlorination and/or chloramination processes (Krasner et al. 2013, Shah and Mitch 2012, Westerhoff and Mash 2002). DON becomes increasingly more important as a result of shorter water cycles through indirect or direct potable reuse leading to higher fractions of wastewaters in source waters used for drinking water production (Krasner et al. 2009, Leverenz et al. 2011, Rodriguez et al. 2009). In addition, climate-related eutrophication and run-off events in upstream agricultural systems have also been identified to impact DON concentrations (Delpla et al. 2009, Graeber et al. 2015, Westerhoff and Mash 2002). Because nitrogen moieties can form hydrogen bonds with the surrounding water molecules, DON moieties can increase the hydrophilic character of NOM (Westerhoff and Mash 2002) making it harder to be removed by conventional treatment processes such as coagulation and filtration. As a result, DON can persist through various non-oxidative treatment schemes and consequently exert oxidant demand and lead to the formation of various measurable nitrogenous oxidation by-products.

Ozone (O_3) can selectively oxidize the electron-rich moieties of DON such as amino acid side chains in polypeptide structures (Sharma and Graham 2010). O_3 reacts with the amine functional groups via adduct formation leading among other products to *N*-oxides for tertiary amines and hydroxylamines for primary and secondary amines (von Sonntag and von Gunten 2012). The adducts can also decay by a series of reaction steps to amine radical cations that subsequently produce dealkylated amines (von Sonntag and von Gunten 2012). Hydroxyl radicals ($^{\bullet}OH$) can also be formed from the reaction of O_3 with DON moieties in addition to other natural or enhanced (e.g., O_3/H_2O_2) O_3 decay processes (von Sonntag and von Gunten 2012).

During ozonation, amino acids play an important role in the reactivity of DON as they can readily react with O_3 through their deprotonated amine nitrogen moiety, with higher second-order rate constants in the presence of methyl, alkyl, or thiol groups (Neta et al. 1988, Sharma and Graham 2010). Glycine, serine, aspartic acid and glutamic acid are the most abundant amino acids in the aquatic environment (Westerhoff and Mash 2002). As reported in a few product studies, amino acids react with O_3 producing nitrate, ammonia, carbonyl and carboxylic acids (Sharma and Graham 2010). Using serine as a model compound, Le Lacheur and Glaze (1996) reported that nitrate and ammonia were among the major end-products of amine nitrogen oxidation under O_3- and $^{\bullet}OH$-dominated conditions, respectively. A study with glycine also showed that the $^{\bullet}OH$ pathway favors ammonia production while O_3 produces nitrate (Berger et al. 1999, Karpel Vel Leitner et al. 2002). In these studies, nitrate formation is induced from the O_3 attack on the amine-nitrogen before cleavage of the C-N bond (Berger et al. 1999, Le Lacheur and Glaze 1996). In contrast, the reaction of $^{\bullet}OH$ leads to a nitrogen-centered radical which rearranges into a C-centered radical analogous to the 1,2-H shift in reactions of alkoxy radicals. This is followed by oxygen addition and loss of superoxide and imine formation, which finally induces a deamination and ammonia production (Berger et al. 1999, Karpel Vel Leitner et al. 2002) (for the mechanism, refer to Fig. S1 of the supporting information). Although the compounds used in these prior studies were smaller molecules than the complex structures of DON moieties, it is worth investigating if the subsequent changes in levels of nitrate and ammonia after ozonation can also occur with differing natural and standard NOM sources. If this is observed, nitrate and ammonia may become important parameters in evaluating the characteristics of an ozonation process such as disinfection efficiency, O_3 exposure (i.e., time integrated concentration of O_3) and contribution of O_3 and $^{\bullet}OH$ to the oxidation. For example, nitrate formed through reactions with O_3 may serve as a surrogate measure for oxidant exposure or disinfection credit (see below for further discussion). Nitrate and ammonia are readily accessible parameters through low cost and low maintenance colorimetric methods (APHA et al. 1999), wherefore, this approach is worth exploring.

This study aims to understand the effect of ozone on DON moieties and the subsequent formation of inorganic nitrogen compounds (NO_3^- and NH_4^+). NOM reference standards, surface water, and wastewater effluent samples were treated under varying ozonation conditions and the changes in nitrate and ammonium concentrations were recorded. Furthermore, the possible major precursors of inorganic nitrogen were identified in experiments using primary, secondary, and tertiary amine model compounds. From the observed results and by using glycine as a model compound, a mechanistic interpretation of the reactions of O_3 with DON was proposed. Lastly, a potential application of the results for characterization of ozonation processes (e.g., estimation of O_3 exposure) were explored.

2. Experimental Methods

2.1. Reagents and chemical analyses

The chemicals used in this study were of reagent grade or higher quality and were purchased from the commercial suppliers shown in Table S1 of the supporting information (SI). All stock solutions were prepared using Milli-Q Direct ultrapure water (18.2 MΩ-cm, Millipore).

Ozonation experiments were performed at the University of Queensland (UQ), Australia and the École Polytechnique Fédérale de Lausanne (EPFL), Switzerland using ozone generated from pure oxygen (99.995%) with an Anseros COM-AD-04 or an Innovatech Type CMG 3-5 ozone generator, respectively. Ozone stock solutions (1 – 1.3 mM O_3) were prepared by sparging O_3-containing oxygen gas through 1 L of ice-bathed MilliQ water and standardized using the absorbance at 260 nm (ε_{260} = 3200 $M^{-1}cm^{-1}$) (von Sonntag and von Gunten 2012). O_3 concentrations in samples were determined by the indigo method (Bader and Hoigné 1981) and O_3 exposure was calculated from the area under the O_3 decay curve (von Gunten and Hoigné 1994). *para*-Chlorobenzoic acid (pCBA) was used as a probe compound for $^{\bullet}OH$ ($k_{^{\bullet}OH+pCBA}$ = 5.0×10^9 $M^{-1}s^{-1}$ (Elovitz and von Gunten 1999)). pCBA concentrations during kinetic experiments were measured using high performance liquid

chromatography (HPLC, Dionex Ultimate 3000, USA) with an acetonitrile/10 mM phosphoric acid mobile phase.

Nitrate was analyzed using a photometric flow injection analyzer (method 31-107-04-1-A, Lachat QuikChem8500, Hach Company, USA) or ion chromatography (ICS 3000, Thermo Scientific, USA) with an eluent KOH (Thermo Scientific Dionex EGC III cartridge). Background nitrite concentrations in the surface and wastewater samples were measured by flow injection analysis (Lachat method 31-107-05-1-A or SEAL method 6-172-96 rev. 15). Nitrite was not found after ozonation of DON because of its high reactivity with O_3 ($k = 5.83\times10^5\ M^{-1}s^{-1}$) (von Sonntag and von Gunten 2012). Ammonium was also analyzed using a Lachat QuikChem (method 31-107-06-1-B) or SEAL analytical autoanalyzer (method 6-171-96 rev. 14, SEAL Analytical, Inc., UK). Methanesulfinic (MSIA) and methanesulfonic acids (MSOA) for $^{\bullet}OH$ yield measurements were quantified by ion chromatography using gradient elution with KOH. Dissolved organic carbon (DOC) and nitrogen were measured using a total organic carbon/nitrogen analyzer (Shimadzu, Japan).

All procedures described in this section are presented in more detail in Text S1-S2, SI, along with method detection limits, standard deviations, and measuring ranges.

2.2. Water samples

Tables S2 – S3 show the characteristics of the water samples used in this study. The surface water sample was taken after coagulation and sedimentation in a drinking water treatment plant in Southeast Queensland (SEQ), Australia. A wastewater effluent sample was obtained from the conventional non-nitrifying Vidy plant in Lausanne, Switzerland. This sample was immediately filtered through a 0.45 μm nylon filter (Membrane Solutions, Switzerland) after collection, and stored at 4 °C until use. NOM standard solutions (10 mg C/L) were prepared using Suwannee River humic acid II (SRHA, 2S101H) and Pony Lake fulvic acid (PLFA, 1R109F) obtained from the International Humic Substances Society (IHSS, MN, USA). These samples were chosen to represent NOM with differing properties.

Synthetic DON solutions containing a mixture of glycine (≥98.5%, Sigma-Aldrich, USA), tannic acid (ACS reagent, Sigma-Aldrich, USA), methanol (MeOH, ≥99.9%, Carlo Erba, Italy) and tertiary butanol (t-BuOH, ≥99.7%, Sigma-Aldrich, Germany) were also used (Table 1). Solutions with trimethylamine (98%, Sigma-Aldrich, USA) and dimethylamine (40% in water, Sigma-Aldrich, USA) as DON source were also prepared (Table 1).

2.3. Experimental conditions

This study was composed of three parts as summarized in Table 1, where the experimental conditions are provided. Further details describing each experiment are available in Text S3 of the supporting information.

Briefly, in the first part, the evolutions of NH_4^+ and NO_3^- in O_3 dosage experiments involving NOM standards (SRHA and PLFA, 10 mg/L DOC), surface water (18 mg/L DOC), and wastewater effluent (6.7 mg/L DOC) at differing conditions were studied. These experiments were carried out by varying the specific O_3 doses and applying treatment conditions that destabilizes (e.g., high pH, addition of radical chain initiators (H_2O_2) and promoters (MeOH)) and stabilizes ozone (e.g., low pH, addition of radical scavengers such as t-BuOH or bicarbonate) (refer to Table 1 for experimental conditions). Table S4 presents the $^{\bullet}OH$ scavenging rates resulting from the use of differing t-BuOH and MeOH concentrations. Kinetic studies to determine O_3 exposure were also conducted using the surface water and wastewater samples.

In the second part, the formation of the inorganic nitrogen species during ozonation (400 μM O_3) of various amines (20 μM each of glycine, dimethylamine, and trimethylamine) was investigated. This was done in the presence of 3 mgC/L tannic acid to mimic phenolic moieties of NOM and to ensure that the amino groups are not the main consumers of O_3 similar to real water samples (Fig. S2). O_3 exposure was controlled by varying concentration ratios of t-BuOH/MeOH. Further explanations on the use of t-BuOH/MeOH for ozone stability control are provided in Text S3.1. These experiments were performed to identify the main amine precursors of NO_3^- and NH_4^+.

The last part of this study involved experiments with glycine as a DON model surrogate. The kinetics of NO_3^- formation during ozonation of glycine-containing water, as well as the $^{\bullet}OH$ yield from the reaction of O_3 with glycine using the dimethylsulfoxide (DMSO) assay (Flyunt et al. 2003, Tekle-Rottering et al. 2016) were investigated. In addition, NO_3^- and NH_4^+ formation from glycine (20 μM) treated for differing ozonation conditions (tannic acid = 3 mgC/L, O_3 dose = 200 – 400 μM, $^{\bullet}OH$ scavenging rates = 1.8×10^5 s^{-1} – 1.3×10^6 s^{-1}) were examined. These experiments (shown in Table 1) aimed to mimic $^{\bullet}OH$ scavenging rates representative for natural systems. Kinetic experiments were also conducted to determine the pseudo-first-order O_3 decay (k_{obs}) constant and R_{ct} (exposure ratio of $^{\bullet}OH$ and O_3) (Elovitz and von Gunten 1999) of each solution (Fig. S3). These parameters are needed for kinetic simulations using the Kintecus software (www.kintecus.com) (Ianni 2003). The k_{obs} and R_{ct} values from each treatment condition were included in the simulation to account for the effect of O_3 stability (e.g., rate of O_3 decay to $^{\bullet}OH$, O_2, and other products) on the elementary reactions of glycine oxidation by O_3. Due to experimental limitations, k_{obs} and R_{ct} for the fast initial ozone consumption were excluded.

All experiments were performed in batch systems by injecting the appropriate volumes of an O_3 stock solution (using a Fortuna Optima glass syringe) into the stirred water samples to reach the desired ozone dose. To maintain a constant pH (± 0.2) during ozonation, the samples were buffered with phosphate (1 – 10 mM) adjusted to the desired pH.

3. Results and Discussion

3.1. Ozonation of DON and formation of inorganic nitrogen compounds

Figure 1 shows the effects of specific ozone doses (gO_3/gDOC) and various ozonation conditions on NO_3^- and NH_4^+ formation from NOM standards (SRHA and PLFA), surface water, and wastewater effluent samples. Overall, it is apparent that NO_3^- generally increases with increasing specific O_3 doses.

For the NOM standards (Fig. 1a), NO_3^- from SRHA (C/N = 44.9 (IHSS 2016)) increased from 0.5 – 1.3 μM for an increase of the specific ozone dose from 0.4 – 1.3 gO_3/gDOC. At the same specific ozone doses, higher yields of NO_3^- were observed for PLFA (1.5 – 4.5 μM) in agreement with the higher relative content of DON (C/N = 8.1 (IHSS 2016)). Figure 1a shows that NH_4^+ in the SRHA experiments did not change significantly while for PLFA, NH_4^+ increased by 75% when increasing the specific O_3 doses from 0.4 to 1.3 gO_3/gDOC. Similar to the results for nitrate, these findings might be explained by the higher nitrogen content of PLFA relative to SRFA.

Previous studies have shown the significance of $^{\bullet}OH$ reactions in driving NH_4^+ formation from amino acids such as glycine (Berger et al. 1999, Karpel Vel Leitner et al. 2002). However, those studies are not comparable to the current study as their $^{\bullet}OH$ transient concentrations were significantly higher because of the use of continuous ozonation (combined with H_2O_2), UV/H_2O_2, or γ-radiolysis. For example, steady-state $^{\bullet}OH$ concentrations of about 5×10^{-12} – 7×10^{-12} M were estimated from a γ-radiolysis study of glycine (i.e., with N_2O or H_2O_2, dose = 2000, 5000, 8000 Gy, average dose rate = 71.6 Gy/min) for reaction times of about 30 – 110 min (Karpel Vel Leitner et al. 2002). In the current study, $^{\bullet}OH$ radicals were only short-lived with expected maximum transient concentrations of about $\leq 10^{-12}$ M (Elovitz and von Gunten 1999). Due to these low $^{\bullet}OH$ concentrations, combined with the low reactivity of amines with $^{\bullet}OH$ at neutral pH (e.g., $k_{(^{\bullet}OH+glycine)}$ = 2.15×10^7 $M^{-1}s^{-1}$ at pH 7 (Buxton et al. 1988)), it is unlikely that $^{\bullet}OH$ from O_3 decay significantly contributes to NH_4^+ formation. Without oxidation by $^{\bullet}OH$, NH_4^+ can be possibly formed from the reaction of O_3 via an electron-transfer pathway to produce *N*-centered radicals and an ozonide (RCH_2-NH_2 + O_3 → RCH_2-$^{\bullet}NH$ + $HO_3^{\bullet}$). The *N*-centered radicals could undergo rearrangement to C-centered radicals (RCH_2-$^{\bullet}NH$ → R-$^{\bullet}CHNH_2$), which in the presence of oxygen form peroxyl radicals (R-$^{\bullet}CHNH_2$ + O_2 → R-($^{\bullet}OO$)$CHNH_2$) (von Sonntag and von Gunten 2012). This is followed by a loss of superoxide, formation of imine intermediates (R-($^{\bullet}OO$)$CHNH_2$ → R-$CH=NH_2^+$ + $O_2^{\bullet-}$), and hydrolysis to NH_4^+ (R-$CH=NH_2^+$ + H_2O → NH_4^+ + R-CHO). For both NOM standards, NO_3^-

concentrations were somewhat lower than NH_4^+ possibly due to rapid O_3 decomposition (i.e., no O_3 residual was measured at the first sampling time of 30 s) leaving insufficient O_3 exposure for oxidation of intermediates to NO_3^-. Because fulvic and humic acid standards may not represent O_3 decomposition kinetics induced by NOM in real waters (Elovitz et al. 2000), further experiments were performed using surface water and wastewater effluent samples.

For the surface water sample (Fig. 1b), differing conditions were used to vary the O_3 exposure including changes of the specific O_3 dose, pH, inorganic carbon, and addition of t-BuOH and/or H_2O_2. The results show that when the specific O_3 doses are increased from 0.4 – 1.0 $gO_3/gDOC$ (corresponding to the typical O_3 doses in SEQ water treatment plants), the NO_3^- concentrations increase, while NH_4^+ concentrations change only slightly. The oxidation of NH_3/NH_4^+ to NO_3^- does not occur under these conditions because of the low reactivity of O_3 with NH_3/NH_4^+ at pH 7 (k_{app} = 9.97×10^{-2} $M^{-1}s^{-1}$, pK_a = 9.3) (Hoigné and Bader 1983, von Sonntag and von Gunten 2012) and low NH_3/NH_4^+ concentration of 0.8 μM. Thus, the observed changes in concentrations of inorganic nitrogen are assumed to result from the reactions of O_3 with DON moieties and the subsequent reactions. Conditions such as a decrease in pH, increase in alkalinity or addition of t-BuOH, which stabilize O_3, resulted in an increase in NO_3^-. In contrast, addition of H_2O_2 leads to a NO_3^- decrease because O_3 is less stable and transformed more quickly to $^{\bullet}OH$ under these conditions. Overall, these observations strongly suggest that O_3 reactions (and not $^{\bullet}OH$) are controlling NO_3^- formation.

The wastewater effluent sample had a very high background NH_3/NH_4^+ concentration of about 1400 μM and a low NO_3^- concentration of 0.5 μM. As such, after ozonation, changes in concentrations were only measureable for NO_3^- and not for NH_4^+. Because of the effluent's high NH_3/NH_4^+ concentrations, NH_3 oxidation was estimated to contribute 32 ± 7% to the observed NO_3^- concentrations (Table S5). The NO_3^- concentrations were then corrected (symbols in Fig. 1c) to show NO_3^- evolution from the ozone oxidation of DON. Generally, similar trends as for the previous water samples were obtained for the corrected NO_3^- concentrations, i.e., increasing NO_3^- for higher specific O_3 doses and for increasing O_3 exposures, which were achieved by increasing the t-BuOH

contribution to the overall $^{\bullet}OH$ scavenging. It should also be noted that the wastewater effluent contained NO_2^- at a concentration of 0.3 μM. However, even for the expected full oxidation of nitrite to nitrate, it has a negligible contribution to the observed NO_3^- levels in the range of 3 – 20 μM. Therefore, the effluent's DON is the major source of NO_3^- during ozonation.

3.2. NO_3^- yields from model compounds (amines)

Some potential precursors of NO_3^- and/or NH_4^+ during ozonation of DON were investigated using the model compounds glycine, dimethylamine, and trimethylamine, representing primary, secondary, and tertiary amines, respectively. The ozone-reactive site for amines is the lone electron pair at the nitrogen atom, with a very low reactivity for protonated amines (von Sonntag and von Gunten 2012). At pH 7, the apparent second-order rate constants of the selected compounds with O_3 (Lee and von Gunten 2010, Neta et al. 1988) are as follows: glycine: $k_{app} = 1.63\times10^2$ $M^{-1}s^{-1}$ (pK_a = 9.3); dimethylamine: $k_{app} = 3.79\times10^3$ $M^{-1}s^{-1}$ (pK_a = 10.7); trimethylamine: $k_{app} = 6.49\times10^3$ $M^{-1}s^{-1}$ (pK_a = 9.8). The higher apparent second-order rate constant of trimethylamine over dimethylamine is due to the former's lower pK_a (von Sonntag and von Gunten 2012) leading to a higher reactive amine fraction (trimethylamine = 0.16%; dimethylamine = 0.02%). During ozonation, O_3 can add to the amine nitrogen forming an O_3-adduct ($R_3N + O_3 \rightarrow R_3N^+OOO^-$), followed by a release of singlet oxygen ($^1O_2$) (Muñoz et al. 2001). For tertiary amines, this reaction leads to an *N*-oxide ($R_3N^+O^-$) formation with high yield, while for primary and secondary amines (e.g., propranolol), the *N*-oxide rearranges to a hydroxylamine (R_2NOH) (Benner and Ternes 2009, von Sonntag and von Gunten 2012). Further oxidation of hydroxylamine can then produce NO_3^-, as observed in the present study.

Figure 2 shows the NO_3^- formation for the selected amines as a function of the $^{\bullet}OH$ scavenging rate. Glycine has the highest NO_3^- yield (i.e., mol NO_3^-/mol amine added) followed by trimethylamine and dimethylamine. At 85% $^{\bullet}OH$ scavenging by t-BuOH, the NO_3^- yield was 85% for glycine, 27% for trimethylamine and 24% for dimethylamine. The highest yield for NO_3^- was obtained for glycine despite having the lowest second-order rate constant for its reaction with O_3 and

281 highest R_{ct} (Table S6). Dimethylamine and trimethylamine solutions had lower R_{ct} values than
282 glycine possibly due to their faster consumption during ozonation, resulting in higher O_3 residual
283 concentrations and hence higher O_3 exposures. The high NO_3^- yield for glycine is due to the fact, that
284 the reactions of primary amines with O_3 nearly exclusively yield NO_3^- as final product (Berger et al.
285 1999), while the reaction with higher substituted amines also gives rise to other stable nitrogen-
286 containing products (Elmghari-Tabib et al. 1982, Muñoz and von Sonntag 2000). For secondary
287 amines such as diethylamine, it was reported that the O_3 reaction occurs predominantly via the
288 formation of an amine-oxyl radical (R_2-$NO^\bullet$, 80%) (von Gunten 2003). From this amine-oxyl radical,
289 nitrone (R_2=N^+O^-) can be formed which hydrolyzes to ethyl hydroxylamine. This product can be
290 further oxidized to NO_3^- in excess of O_3 (von Gunten 2003). The slightly higher NO_3^- yield of
291 trimethylamine compared to dimethylamine could be a result of the compound's higher apparent
292 second-order rate constant and the predominance of oxygen transfer (*N*-oxide formation) over
293 electron-transfer reactions (amine radical cation formation). The predominance of *N*-oxide formation
294 has also been shown for other tertiary amines such as ethylenediamine tetraacetic acid (EDTA),
295 nitrilotriacetic acid (NTA), tramadol, and clarithromycin (Lange et al. 2006, Muñoz and von Sonntag
296 2000, Zimmermann et al. 2012).

297 In our experiment, NH_4^+ from electron-transfer reactions was only observed for glycine (0.6 –
298 1.2 μM, equivalent to yields of 3% – 6% μM NH_4^+/μM glycine added). No NH_4^+ was detected for
299 dimethylamine and trimethylamine because of the higher degree of alkylation. The hydrolysis of the
300 imine intermediate would consequently result in lower substituted amines (e.g., tertiary to secondary
301 amines (Muñoz and von Sonntag 2000)) instead of NH_4^+.

302 *3.3. NO_3^- formation kinetics from glycine*

303 To further elucidate NO_3^- formation from glycine, ozonation was performed with solutions
304 containing glycine and t-BuOH (complete scavenging of $^\bullet$OH). As shown in Fig. 3a, upon ozonation,
305 the simulated glycine concentration decreases rapidly (pH 7: $k_{gly,O3}$ = 1.63×10^2 $M^{-1}s^{-1}$, $t_{1/2}$ =
306 $0.69/(k_{gly,O3}\int[O_3]dt)$ = 0.02 s), while the measured NO_3^- increases only slowly. This indicates that

307 NO_3^- is produced from an intermediate species (referred to as X) and not directly from glycine. The
308 rate of NO_3^- formation therefore depends on further oxidation of X. Assuming 100% conversion of
309 glycine to X during ozonation, X_{max} (the maximal yield of X after glycine decomposition) can be
310 estimated equal to $[glycine]_0$. Thus, X at time t (X_t) is equal to X_{max} minus NO_3^- and the rate constant
311 for X abatement can be calculated using second-order kinetics. Plotting $\ln[X]_t/[X]_{max}$ versus O_3
312 exposure yields a linear plot (Fig. S4) with a slope equal to the second-order rate constant of
313 ozonation of X (k = 7.7 ± 0.1 $M^{-1}s^{-1}$), which corresponds to the formation of NO_3^-. Using this value,
314 the experimentally measured NO_3^- was predicted relatively well (dotted line in Fig. 3a) using kinetic
315 simulations involving the following reactions: O_3 + glycine → hydroxylamine (k_{app} = 1.63×10^2 $M^{-1}s^{-1}$
316 (Neta et al. 1988), hydroxylamine + O_3 → X (k_{app} = 2×10^4 $M^{-1}s^{-1}$ (Hoigné et al. 1985)), X + O_3 →
317 NO_3^- (k_{app} = 7.7 $M^{-1}s^{-1}$), and O_3 → products (experimental first-order O_3 decay = 1.57×10^{-3} s^{-1}). The
318 NO_3^- yield at full O_3 consumption (~50 min) showed a nearly complete mineralization of glycine to
319 NO_3^-. Based on the mechanistic discussion below, the oxime ($HON=CHCO_2^-$) formed during further
320 oxidation of hydroxylamine may be a good candidate for X. This hypothesis, however, needs to be
321 validated in future studies.

322 *3.4. $^{\bullet}OH$ yield from the reaction of ozone with glycine*

323 Figure 3b shows the NH_4^+ formed when excess of glycine (100 mM) was treated with 0.1 – 0.4
324 mM O_3. In contrast to previous product studies with glycine (Berger et al. 1999), NH_4^+ in the current
325 study is not formed from the reaction of glycine with $^{\bullet}OH$. This is because at pH 7, the apparent
326 second-order rate constant for the reaction of glycine with $^{\bullet}OH$ is only 2.15×10^7 $M^{-1}s^{-1}$ (Buxton et al.
327 1988), which is very low compared to commonly encountered diffusion-controlled second-order rate
328 constants for reactions with $^{\bullet}OH$ (>10^9 $M^{-1}s^{-1}$). Based on this low reactivity and the low steady-state
329 $^{\bullet}OH$ concentrations, NH_4^+ formation by this pathway can be excluded during ozonation. Instead, we
330 propose that NH_4^+ is produced through an electron-transfer pathway involving ozone. This pathway
331 proceeds via an ozone adduct intermediate ($R\text{-}NH_2^+OOO^-$) (von Sonntag and von Gunten 2012), a

subsequent *N*-centered radical formation followed by C-N H-shift, oxygen addition to the C-centered radical, and loss of superoxide ($O_2^{\bullet-}$) (refer to Fig. 6, reactions 1,7, 13-15). These reactions would result in an imine intermediate that can hydrolyze to NH_4^+. The $O_3^{\bullet-}$ and $O_2^{\bullet-}$ associated with these reaction steps cause $^{\bullet}OH$ formation. For $O_3^{\bullet-}$, $^{\bullet}OH$ can be formed from the subsequent rapid equilibria of $O_3^{\bullet-} \leftrightarrow O^{\bullet-} + O_2$ and $O^{\bullet-} + H_2O \leftrightarrow {}^{\bullet}OH + OH^-$ (Merenyi et al. 2010) whereas for $O_2^{\bullet-}$, $^{\bullet}OH$ can be formed from its reaction with O_3 yielding $O_3^{\bullet-}$ (von Sonntag and von Gunten 2012). Since the formation of NH_4^+ and $^{\bullet}OH$ occurs simultaneously, a linear correlation between the two parameters is observed (Fig. 3b).

Furthermore, the $^{\bullet}OH$ yield from ozonation of glycine was determined using the DMSO assay (Fig. 3c). The $^{\bullet}OH$ yield for glycine was calculated to be 24.7 ± 1.9% (mol $^{\bullet}OH$/mol O_3 consumed), which means that about 25% of the consumed O_3 produces $^{\bullet}OH$ and possibly NH_4^+. The $^{\bullet}OH$ yield is within the range determined for triethylamine (15%) (Flyunt et al. 2003) and piperidine (28%) (Tekle-Rottering et al. 2016). Unfortunately, data for $^{\bullet}OH$ yields for other primary aliphatic amines is lacking in literature limiting the options for comparison with previous studies. The measured $^{\bullet}OH$ formation confirms that an electron-transfer mechanism occurs during ozonation of glycine. A plot of the NH_4^+ against the $^{\bullet}OH$ concentration (Fig. 3b) gives a linear correlation with a slope of 0.03 mol NH_4^+/mol $^{\bullet}OH$, which means that the measured NH_4^+ concentrations are much lower than expected from the $^{\bullet}OH$ formed. This is a strong indication that other reactions producing $^{\bullet}OH$ compete with NH_4^+ formation.

3.5. NO_3^- and NH_4^+ formation during ozonation of synthetic waters mimicking realistic conditions

Ozonation experiments with synthetic DON solutions (20 μM glycine + 3 mgC/L tannic acid + t-BuOH/MeOH) were performed with two $^{\bullet}OH$ scavenging rates, which are about a factor of 10 apart (high: 1.3×10^6 s^{-1} (Figs. 4a and 4b) and low: 1.8×10^5 s^{-1} (Figs. 4c and 4d)). The first set of experiments was performed using the high $^{\bullet}OH$ scavenging conditions with t-BuOH/MeOH (μM/μM) ratios of 417/1000 – 1875/125. Under these conditions, R_{ct} values of 9.70×10^{-10} – $1.95 \times 10^{-}$

^{8} were measured for O_3 doses of 200 – 400 μM. To evaluate the formation of inorganic nitrogen compounds over a wider range of R_{ct}s, the concentrations of t-BuOH/MeOH were decreased 12.5 times resulting in water samples with lower $^{\bullet}OH$ scavenging rates. Therefore, in the second set of experiments, using the same O_3 doses, higher R_{ct} values (2.03×10^{-8} – 1.55×10^{-7}) were obtained. Overall, R_{ct} values (summarized in Tables S8 and S10) covered a realistic range of 10^{-10} – 10^{-7}, which are within the range of R_{ct}s reported in various types of water samples and for various treatment conditions (Acero and von Gunten 2001, Elovitz et al. 2000, Shin et al. 2015).

NO_3^- increased with increasing O_3 doses for all experimental conditions (Figs. 4a and 4c). For an 85% $^{\bullet}OH$ scavenging by t-BuOH, NO_3^- increased from 3.6 – 10.6 μM when increasing the O_3 dose from 200 – 400 μM (Fig. 4a). A similar trend was also observed at 50% $^{\bullet}OH$ scavenging by t-BuOH (Fig. 4c) where NO_3^- increased from 3.3 – 8.5 μM for the same increase in O_3 doses (200 – 400 μM). Several subsequent O_3 reactions play a major role in the formation of NO_3^-, as demonstrated by an increase in NO_3^- concentrations for increasing %$^{\bullet}OH$ scavenging by t-BuOH. For NH_4^+, higher concentrations were observed at lower O_3 doses and only slight changes in concentrations were observed at varying t-BuOH concentrations (Figs. 4b and 4d). The latter observation supports our hypothesis that the contribution of $^{\bullet}OH$ reactions to the overall NH_4^+ formation can be neglected. At lower O_3 doses, higher NH_4^+ concentrations were observed because of the fast initial O_3 reactions (e.g., electron-transfer and radical chain reactions) forming intermediates that are reactive to the remaining O_3 and O_2 in the solution, consequently producing amides and NH_4^+, respectively (for mechanistic discussion, see below). Briefly, O_3 can also react with C-centered radicals, however, such reactions would lead to an alkoxyl radical (von Sonntag and von Gunten 2012) that will give rise to an amide (not an imine and subsequently NH_4^+). Thus, in the context of NH_4^+ formation, O_3 is only important at the initial electron-transfer step while residual O_3 will compete with O_2 for the C-centered radical. This competition reaction could cause the observed higher NH_4^+ concentration at lower O_3 dose (Figs. 4b and 4d). Because O_2 is high in ozonated solutions, a decrease in available O_3

would promote O_2 reactions with C-centered radicals that eventually lead to NH_4^+ formation (see below).

3.6. Relationship between O_3 exposure and NO_3^- formation

So far, it was clearly demonstrated that the NO_3^- formation is sensitive to changes in ozonation conditions for all investigated water samples. For the applied conditions, it was consistently observed that NO_3^- increases with increasing O_3 doses and exposures. A summary of all the related data is presented in Fig. 5. A similar trend was previously reported, e.g., during continuous ozonation of glycine with decreasing H_2O_2 and increasing bicarbonate concentrations (Berger et al. 1999). However, in the previous study, O_3 exposures were not measured. In the current study, linear relationships ($R^2 \geq 0.82$) were observed between NO_3^- concentrations and O_3 exposures in glycine-containing solutions (both at high and low $^{\bullet}OH$ scavenging), surface water and wastewater samples (Figs. 5a – 5d). This direct relationship applies to a wide range of O_3 exposure (~0 – 0.12 Ms (equivalent to 0 – 96 mg/L·min)), with slopes extending from 51 µM/Ms in surface water to 166 µM/Ms in secondary wastewater effluent. Standard NOM solutions were not included because of the limitation in measuring the fast O_3 decomposition. These results indicate that NO_3^- formation depends on the O_3 exposure, which is a measure for the primary and subsequent O_3 reactions with amine moieties in DON. This also suggests that the conversion of amines to readily oxidizable intermediates and NO_3^- is a relatively straightforward process in the presence of O_3. Intermediates such as hydroxylamines and oximes are expected, as seen in other ozonation studies of amines (Elmghari-Tabib et al. 1982), which can be further oxidized to NO_3^- and the corresponding carbonyl compounds (e.g., glyoxylic acid).

3.7. Mechanistic interpretations

The proposed reactions in the glycine-ozone system are summarized in Fig. 6. They are based on the following observations from this study: (a) NO_3^- increases with increasing O_3 exposures, (b) NO_3^- is produced from an oxidized glycine intermediate, (c) there is an almost 100% conversion of glycine to NO_3^- in excess of O_3 and for complete $^{\bullet}OH$ scavenging by t-BuOH, (d) NH_4^+ yields were higher at

lower O_3 doses, (e) the O_3 reaction with glycine has a $^{\bullet}OH$ yield of about 25%, and (f) significantly lower NH_4^+ concentrations were observed than expected from the $^{\bullet}OH$ yield.

Ozone reacts with glycine with the formation of an O_3 adduct (reaction 1) which can decompose to an *N*-oxide (reaction 2) and an aminyl radical (reaction 7). The *N*-oxide can then rearrange to monohydroxylamine (reaction 3) (von Sonntag and von Gunten 2012), which leads to dihydroxylamine (reaction 4) upon further oxidation by O_3. Dehydration then forms an oxime (reaction 5) that produces NO_3^- and glyoxylic acid (reaction 6) in the presence of O_3. This series of reactions is based on previously reported pathways by Berger et al. (1999).

Electron-transfer reactions are responsible for the formation of a *N*-centered radical species (reactions 7) (von Sonntag and von Gunten 2012). *N*-centered radicals were reported for similar reactions by Bonifacic et al. (1998) although they used $^{\bullet}OH$ as the oxidant and not O_3. Nevertheless, such types of reactions are plausible for our system as suggested by the measured $^{\bullet}OH$ formation (section 3.4).

O_3 can react with the aminyl radical (reaction 8) to form a *N*-oxyl radical after loss of singlet oxygen (reaction 9). The *N*-oxyl radical undergoes a dismutation (reaction 10) (Jayson et al. 1955) to form an oxime and hydroxylamine that can also form NO_3^- upon further oxidation (reaction 11). This reaction is in competition with reaction of O_3 with the *N*-oxyl radical leading to a *N*-centered radical and oxygen (reaction 12). To produce NH_4^+ over the reaction sequence initiated by reaction 7, a C-N H-shift (reaction 13) from the aminyl radical can occur resulting in a C-centered radical (Bonifacic et al. 1998, von Sonntag and von Gunten 2012). Since the reaction occurs in presence of O_2, a peroxyl radical can be produced (reaction 14) (Abramovitch and Rabani 1976, Neta et al. 1990) followed by a release of $O_2^{\bullet-}$ to form an imine intermediate (reaction 15) (von Sonntag and Schuchmann 1991). This product can then hydrolyze to NH_4^+ and glyoxilic acid (reaction 16). Another side reaction can happen through the bimolecular decay of the peroxyl radical forming a tetroxide intermediate (i.e., Bennett- and Russell-type mechanism, reaction 17) (von Sonntag and von Gunten 2012) and eventually oxamic acid (reaction 18) (Berger et al. 1999, Karpel Vel Leitner et al. 2002). Competing

434 with the peroxyl radical formation is the reaction of O_3 with the C-centered radical forming an
435 adduct (reaction 19). This adduct is highly unstable consequently releasing O_2 thereby leading to an
436 alkoxyl radical (reaction 20) (von Sonntag and von Gunten 2012). This can be followed by a 1,2-H
437 shift reaction (Konya et al. 2000) (reaction 21), O_2 addition to form an α-hydroxyperoxyl radical
438 (reaction 22), and loss of $HO_2^{\bullet}$ to also form oxamic acid (reaction 23). These reactions seem to be
439 quite important in the investigated reaction system because NH_4^+ concentrations were higher at lower
440 O_3 doses suggesting less competition with O_2 for NH_4^+ formation. Based on these reactions, the
441 lower NH_4^+ concentrations compared to the formation of $^{\bullet}OH$ (section 3.4) could be caused by: (a)
442 reaction of O_3 with RCH_2-$^{\bullet}NH$ to form NO_3^- (reactions 8 – 11), (b) decay of peroxyl radicals through
443 a tetroxide leading to oxamic acid (reactions 17 – 18), and (c) reaction of O_3 with R-$^{\bullet}CHNH_2$
444 through an alkoxyl intermediate that also forms oxamic acid (reactions 19 – 23).

445 *3.8. Kinetic simulations of experimental data from model systems*

446 A kinetic model was set up to simulate the experimental data in Fig. 4. The symbols are
447 experimental results and the lines are derived from kinetic simulations using the reactions (RS) and
448 rate constants listed in Table S11. The second column of Table S11 shows the corresponding
449 reactions shown in Fig. 6.

450 The model accounts for the reaction of glycine with O_3 via oxygen- and electron-transfer. It is
451 mainly composed of 3 components: (1) NO_3^--forming reactions (RS1-RS3, RS5-RS6), (2) NH_4^+-
452 forming reactions and corresponding competing reactions (RS4, RS8-RS14), and (3) O_3
453 decomposition reactions (RS15-RS17). A reasonable agreement with the experimental results was
454 obtained for NO_3^- both for high and low $^{\bullet}OH$ scavenging rates (Figs. 4a and 4c). This suggests that
455 the rate constants and reactions considered are reasonable to predict NO_3^- formation. Since the model
456 includes measured and estimated rate constants, and measurements of R_{ct} and O_3 decay constants, the
457 observed deviation of the model from the experimental data are not astonishing. Nevertheless, the
458 model was able to show trends which are consistent with the experimentally determined NO_3^-
459 concentrations.

460 In the model, NO_3^- is formed from an intermediate (assumed to be $HON=CHCO_2^-$) by RS3
461 (Table S11; see section 3.3) with a second-order rate constant of 7.7 $M^{-1}s^{-1}$ (Fig. S4). This reaction is
462 preceded by RS1 (O-transfer to N, producing a hydroxylamine) and RS2 (ozonation of
463 hydroxylamine). RS2 was included since hydroxylamines are among the known products of
464 ozonation of primary amines (k_{RS2} = 2.0×10^4 $M^{-1}s^{-1}$) (Hoigné et al. 1985). It can also be seen that RS1
465 is in competition with RS4, which accounts for electron-transfer reaction. The second-order rate
466 constant used for RS1 was equal to 1.23×10^2 $M^{-1}s^{-1}$, 75% of the known second-order rate constant
467 for the reaction of glycine with O_3 at pH 7 (k = 1.63×10^2 $M^{-1}s^{-1}$) (Lee and von Gunten 2010, Neta et
468 al. 1988). This fraction was used because a 25% $^{\bullet}OH$ yield was measured from the ozone-glycine
469 reaction (section 3.4). Considering that $^{\bullet}OH$ can be formed from ozonide in reaction 7, a second-
470 order rate constant of 41 $M^{-1}s^{-1}$ was assigned for electron-transfer reactions (RS4). The relatively
471 good agreement of the model and the experimental data supports the mechanistic assumptions in this
472 study.

473 The *N*-centered radical, $HN^{\bullet}$-$CH_2CO_2^-$, would react directly with O_3 and indirectly with O_2 after
474 rearrangement to the corresponding C-centered radical. Since we found earlier that glycine can be
475 completely converted to NO_3^- (section 3.3), it is highly possible that NO_3^- can also form from
476 reactions involving the *N*-centered radical. O_3 addition to $HN^{\bullet}$-$CH_2CO_2^-$ leads to an *N*-oxyl radical
477 (RS5) with subsequent dismutation reaction (RS6). This results in products such as hydroxylamine
478 and oxime that forms NO_3^- by further oxidation. Rate constants for the reaction of aminyl radicals
479 with ozone are still unknown. But for the simulation, a second-order rate constant of 3.0×10^9 $M^{-1}s^{-1}$
480 (i.e., close to diffusion-controlled reactions) was assumed to fit the experimental data. For the
481 dismutation of the *N*-oxyl radicals (RS6), a rate constant of 1.0×10^9 $M^{-1}s^{-1}$ was assigned which is
482 typical for radical-radical reactions (Buxton et al. 1988). The *N*-oxyl radical can also react with O_3
483 (RS7) to form another *N*-centered radical, similar to those reported for TEMPO (k = 1.3×10^7 $M^{-1}s^{-1}$)
484 (von Sonntag and von Gunten 2012).

In another pathway, rearrangement of $HN^{\bullet}\text{-}CH_2CO_2^-$ to $H_2N\text{-}^{\bullet}CHCO_2^-$ (RS8; $k = 2.0\times10^6$ s^{-1} based on 1,2-H shift in alkoxy radicals in RS10) results in reactions with O_3 (to oxamic acid) and O_2 (to NH_4^+) (RS9 – RS14). O_2 addition to $H_2N\text{-}^{\bullet}CHCO_2^-$ results in peroxyl radicals (RS12) that could decay via elimination of $O_2^{\bullet-}$ (RS13) forming an imine that hydrolyzes to NH_4^+, and/or a tetroxide (Bennett mechanism) forming an amide as the final product (RS14). Because of the relatively similar addition reactions of O_3 ($RC\text{-}OOO^{\bullet}$) and O_2 ($RC\text{-}OO^{\bullet}$) for C-centered radicals, second-order rate constants of 1×10^9 – 3×10^9 $M^{-1}s^{-1}$ were assigned for RS9, RS11, and RS12. These rate constants are typical for reactions of C-centered radicals with O_2 and O_3 (Maillard et al. 1983, Neta et al. 1990, von Sonntag and von Gunten 2012). It should be noted that RS9 (reactions 19-20) has a strong influence in NH_4^+ formation. Decreasing its second-order rate constant overestimates the NH_4^+ due to insufficient competition with RS12 (reaction 14). Peroxyl radicals derived from glycine eliminate $O_2^{\bullet-}$ (RS13) with a first-order rate constant of 1.5×10^5 s^{-1} (Neta et al. 1990), whereas their bimolecular decay (RS14) can occur with a second-order rate constant of about 1.0×10^9 $M^{-1}s^{-1}$ which is similar to the decay of most primary peroxyl radicals (Neta et al. 1990, von Sonntag 2006). Although the predicted values for NH_4^+ fall within the range of experimental values, the deviations from the predicted values suggest the possibility of other unknown reactions involving C- and *N*-centered radicals that are not considered in Table S11.

The actual O_3 decay characteristics in the synthetic water samples were incorporated using R_{ct} and O_3 decomposition reactions (RS15 – RS17). The elementary reactions for ozone decomposition can lead to formation of ozonide radical that gives rise to $^{\bullet}OH$ and O_2 as main products (RS15 and RS17) (Merenyi et al. 2010, Pocostales et al. 2010). As can be seen in Fig. 4, even at differing conditions (O_3 dose and $\%^{\bullet}OH$ scavenging by t-BuOH), the simulation can effectively describe the formation of inorganic nitrogen species provided that R_{ct} and O_3 decay constants are measured for each experimental condition. These constants constitute an integral part of the model because they account for the decay kinetics of O_3 used in reactions RS1-RS5, RS7, and RS9. The experimental

first-order O_3 decay constants and R_{ct} values are presented in Tables S7 – S10. Initial O_2 concentrations of 0.28 mM (9 mg/L O_2) were used to mimic the dissolved O_2 at ambient conditions (20 °C, 1 bar) (USGS 2014).

3.9. Practical implications

This study gives evidence that formation of inorganic nitrogen species is greatly influenced by the ozonation conditions of a water sample. One practical application of the results would be in the context of assessment of oxidation/disinfection efficiency during ozonation. Since a strong correlation was found between NO_3^- and O_3 exposure (Fig. 5), water utilities could continuously monitor NO_3^- concentrations to evaluate if their treatment plant achieves a required O_3 exposure or CT for disinfection or for oxidation of micropollutants. This can be achieved by initial calibrations of the ozonation process with NO_3^- formation, i.e., a measured increase in the NO_3^- level would correspond to a certain O_3 exposure. This approach might be applicable to a wide range of conditions as the direct correlation of NO_3^- concentrations with O_3 exposures applies for different water samples with R_{ct}s ranging from 10^{-10} – 10^{-7}. Hence, the measurement of NO_3^- could be a useful parameter to alert operators that likely a water quality change has occurred in the treatment plant when the detected NO_3^- concentrations deviate from typically observed levels. For example, waters that show a sudden increase in NO_3^- concentration despite having the same ozonation conditions could indicate that there is a significant change in the quantity and quality of the influent DON. Similarly, an increase in NH_4^+ and decrease in NO_3^- concentrations could suggest having lower O_3 exposures and that higher ozone doses might be needed to achieve the desired disinfection credit. Thus, these results may be useful to complement the monitoring tools currently applied in water treatment to assess O_3 exposures.

However, the new concept that we presented also has limitations. For example, the changes in NO_3^- with O_3 exposure was not very apparent when ozonation pH was varied (Fig. S5). This is due to the contrasting effects of O_3 exposure and reactivity of amines at differing pH. Despite the increase in O_3 exposure at lower pH, decreasing the pH from 8 to 6 would result in a 100-fold decrease in the

rate constant of glycine with O_3. Thus, pH needs to be taken into account, when designing an algorithm based on the present findings to monitor O_3 exposure. In addition, since this approach relies on measuring changes in inorganic nitrogen, the necessary high instrument precision is required. This is problematic in at least two instances. For example, measurement of DON oxidation in a drinking water source in Lausanne (Lake Geneva), Switzerland was not possible due to the low initial NOM concentration (DOC = 0.85 mg/L). Typical C:N ratios in natural water (~15 mgC/mgN) (Westerhoff and Mash 2002) would put the DON at 0.06 mg/L or less which is well below the instrument detection limit. In contrast, a very high background inorganic nitrogen concentration before ozonation may also pose challenges to the analytical determination of the formation of NO_3- and/or NH_4^+.

4. Conclusions

The reactions between O_3 and DON in real water samples, standard NOM sources, and model DON solutions (e.g., glycine) were investigated. The following conclusions can be drawn from this study:

- NO_3^- and NH_4^+ concentrations vary with changing ozonation conditions in model DON solutions (e.g., glycine) as well as in real water samples (e.g., surface water and wastewater effluent). Increasing NO_3^- concentrations were observed with increasing O_3 doses while the opposite applies for NH_4^+. A direct correlation between NO_3^- and O_3 exposure was apparent for the tested synthetic and natural water samples. Primary amines were found to be a potential precursor for NO_3^- and NH_4^+ formation during ozonation.
- NO_3^- formation during ozonation of glycine occurs via an oxygen-containing intermediate from the oxidation of glycine. To form NO_3^-, an O_3 adduct is formed followed by hydroxylamine formation, which upon further oxidation leads to an oxime and finally NO_3^-.

- For the ozonation conditions in this study, $^{\bullet}OH$ reactions with glycine can be neglected due to the low transient $^{\bullet}OH$ concentrations and the low reactivity of amines at neutral pH. NH_4^+ formation is hypothesized to occur through an electron-transfer reaction involving O_3, which produce $O_3^{\bullet-}$ and C-centered radicals that subsequently react with O_2. The resulting intermediates (e.g., imine compounds) consequently hydrolyze to NH_4^+. This pathway was confirmed from the measured $^{\bullet}OH$ formed from subsequent reactions of $O_3^{\bullet-}$ and $O_2^{\bullet-}$. An $^{\bullet}OH$ yield of 25% was determined from the ozone-glycine reaction.

Acknowledgements

This study was funded by a collaboration with Seqwater (Australia), the Water Research Foundation (project WRF #4484), and the Water Quality and Treatment Laboratory of EPFL (Switzerland). G.A.D. de Vera is grateful of the Australia Awards PhD scholarship, UQ International scholarship, and UQ Graduate School International Travel Award. Dr. Maria José Farré acknowledges the European Commission for funding project 623711 under the FP7-PEOPLE-2013-IIF - Marie Curie Action: "International Incoming Fellowships". Thanks also to Minju Lee and Michèle Heeb for helpful discussions. Beatrice Keller-Lehmann, Sylvain Coudret, Florian Breider and Caroline Gachet are acknowledged for their laboratory assistance.

References

Abramovitch, S. and Rabani, J. (1976) Pulse radiolytic investogations of peroxyl radicals in aqueous solutions of acetate and glycine. J. Phys. Chem. 80(14), 1562-1565.

Acero, J.L. and von Gunten, U. (2001) Characterization of oxidation processes: Ozonation and the AOP O_3/H_2O_2. J. Am. Water Works Ass. 93(10), 90-100.

APHA, AWWA and WEF (1999) Standard methods for the examination of water and wastewater.

Bader, H. and Hoigné, J. (1981) Determination of ozone in water by the indigo method. Water Res. 15, 449-456.

586 Benner, J. and Ternes, T.A. (2009) Ozonation of propranolol: formation of oxidation products.
587 Environ. Sci. Technol. 43, 5086-5093.
588 Berger, P., Karpel Vel Leitner, N., Dore, M. and Legube, B. (1999) Ozone and hydroxyl radicals
589 induced oxidation of glycine. Water Res. 33(2), 433-441.
590 Bonifacic, M., Stefanic, I., Hug, G.L., Armstrong, D.A. and Asmus, K.-D. (1998) Glycine
591 decarboxylation: the free radical mechanism. J. Am. Chem. Soc. 120, 9930-9940.
592 Buxton, G.V., Greenstock, C.L., Helman, W.P. and Ross, A.B. (1988) Critical review of rate
593 constants for reactions of hydrated electrons, hydrogen atoms, and hydroxyl radicals (•OH/•O-) in
594 aqueous solution. J. Phys. Chem. Ref. Data 17(2).
595 Delpla, I., Jung, A.V., Baures, E., Clement, M. and Thomas, O. (2009) Impacts of climate change on
596 surface water quality in relation to drinking water production. Environ. Int. 35(8), 1225-1233.
597 Elmghari-Tabib, M., Laplanche, A., Venien, F. and Martin, G. (1982) Ozonation of amines in
598 aqueous solutions. Water Res. 16, 223-229.
599 Elovitz, M.S. and von Gunten, U. (1999) Hydroxyl radical/ozone ratios during ozonation processes.
600 I. the Rct concept. Ozone-Sci. Eng. 21(3), 239-260.
601 Elovitz, M.S., von Gunten, U. and Kaiser, H.-P. (2000) The influence of dissolved organic matter
602 character on ozone decomposition rates andRct. In Natural Organic Matter and Disinfection By-
603 Products; Barrett, S., et al.; ACS Symposium Series; American Chemical Society: Washignton,
604 DC. 761, 248-269.
605 Flyunt, R., Leitzke, A., Mark, G., Mvula, E., Reisz, E., Schick, R. and von Sonntag, C. (2003)
606 Determination of $^{\bullet}OH$, $O_2^{\bullet-}$, and hydroperoxide yields in ozone reactions in aqueous solution. J.
607 Phys. Chem. B 107, 7242-7253.
608 Graeber, D., Boechat, I.G., Encina-Montoya, F., Esse, C., Gelbrecht, J., Goyenola, G., Gucker, B.,
609 Heinz, M., Kronvang, B., Meerhoff, M., Nimptsch, J., Pusch, M.T., Silva, R.C., von Schiller, D.
610 and Zwirnmann, E. (2015) Global effects of agriculture on fluvial dissolved organic matter. Sci.
611 Rep. 5, 16328.

612 Hoigné, J. and Bader, H. (1983) Rate constants of reactions of ozone with organic and inorganic
613 compounds in water II. Dissociating organic compounds. Water Res. 17, 185-194.
614 Hoigné, J., Bader, H., Haag, W.R. and Staehelin, J. (1985) Rate constants of reactions of ozone with
615 organic and inorganic compounds in water - III. Inorganic compounds and radicals. Water Res.
616 19(8), 993-1004.
617 Ianni, J.C. (2003) A comparison of the Bader-Deuflhard and the Cash-Karp Runge-Kutta integrators
618 for the GRI-MECH 3.0 model based on the chemical kinetics code Kintecus. In: Bathe, K.J. (Ed.),
619 Computational Fluid and Solid Mechanics. Elsevier, Amsterdam, pp. 1368–1372.
620 IHSS (2016) Elemental compositions and stable isotopic ratios of IHSS samples. Available at
621 http://www.humicsubstances.org/elements.html.
622 Jayson, G.G., Scholes, G. and Weiss, J. (1955) Chemical action of ionising radiations in solution.
623 Part XIV. The action of X-rays (200 kv) on some aliphatic amines in aqueous solution with
624 particular reference to the formation of oximes. J. Chem Soc., 2594-2600.
625 Karpel Vel Leitner, N., Berger, P. and Legube, B. (2002) Oxidation of amino groups by hydroxyl
626 radicals in relation to the oxidation degree of the a-carbon. Environ. Sci. Technol. 36, 3083-3089.
627 Konya, K.G., Paul, T., Lin, S., Lusztyk, J. and Ingold, K.U. (2000) Laser flash photolysis studies on
628 the first superoxide thermal source. First direct measurements of the rates of solvent-assisted 1,2-
629 hydrogen atom shift and a proposed new mechanism for this unusual rearrangement. J. Am.
630 Chem. Soc. 122, 7518-7527.
631 Krasner, S.W., Mitch, W.A., McCurry, D.L., Hanigan, D. and Westerhoff, P. (2013) Formation,
632 precursors, control, and occurrence of nitrosamines in drinking water: a review. Water Res.
633 47(13), 4433-4450.
634 Krasner, S.W., Westerhoff, P., Chen, B., Rittmann, B.E., Nam, S.-N. and Amy, G. (2009) Impact of
635 wastewater treatment processes on organic carbon, organic nitrogen, and DBP Precursors in
636 effluent organic matter. Environ. Sci. Technol. 43(8), 2911-2918.

637 Lange, F., Cornelissen, S., Kubac, D., Sein, M.M., von Sonntag, J., Hannich, C.B., Golloch, A.,
638 Heipieper, H.J., Moder, M. and von Sonntag, C. (2006) Degradation of macrolide antibiotics by
639 ozone: A mechanistic case study with clarithromycin. Chemosphere 65(1), 17-23.
640 Le Lacheur, R.M. and Glaze, W.H. (1996) Reactions of ozone and hydroxyl radicals with serine.
641 Environ. Sci. Technol. 30, 1072-1080.
642 Lee, Y. and von Gunten, U. (2010) Oxidative transformation of micropollutants during municipal
643 wastewater treatment: comparison of kinetic aspects of selective (chlorine, chlorine dioxide,
644 ferrate VI, and ozone) and non-selective oxidants (hydroxyl radical). Water Res. 44(2), 555-566.
645 Leverenz, H.L., Tchobanoglous, G. and Asano, T. (2011) Direct potable reuse: a future imperative. J.
646 Water Reuse Desal. 1(1), 2-10.
647 Maillard, B., Ingold, K.U. and Scaiano, J.C. (1983) Rate constants for the reaction of free radicals
648 with oxygen in solution. J. Am. Chem. Soc. 105(15), 5095-5099.
649 Merenyi, G., Lind, J., Naumov, S. and von Sonntag, C. (2010) Reaction of ozone with hydrogen
650 peroxide (peroxone process): a revision of current mechanistic concepts based on thermokinetic
651 and quantum-chemical considerations. Environ. Sci. Technol. 44, 3505-3507.
652 Muñoz, F., Mvula, E., Braslavsky, S.E. and von Sonntag, C. (2001) Singlet dioxygen formation in
653 ozone reactions in aqueous solution. J. Chem. Soc., Perkin Trans. 2 (7), 1109-1116.
654 Muñoz, F. and von Sonntag, C. (2000) The reactions of ozone with tertiary amines including the
655 complexing agents nitrilotriacetic acid (NTA) and ethylenediaminetetraacetic acid (EDTA) in
656 aqueous solution. J. Chem. Soc., Perkin Trans. 2 (10), 2029-2033.
657 Neta, P., Huie, R.E. and Ross, A.B. (1988) Rate constants for reactions of inorganic radicals in
658 aqueous solution. J. Phys. Chem. Ref. Data 17(3), 1027-1284.
659 Neta, P., Huie, R.E. and Ross, A.B. (1990) Rate constants for reactions of peroxyl radicals in fluid
660 solutions. J. Phys. Chem. Ref. Data 19(2), 413.
661 Pocostales, J.P., Sein, M.M., Knolle, W., von Sonntag, C. and Schmidt, T.C. (2010) Degradation of
662 ozone-refractory organic phosphates in wastewater by ozone and ozone/hydrogen peroxide

(peroxone): The role of ozone consumption by dissolved organic matter. Environ. Sci. Technol. 44, 8248-8253.

Rodriguez, C., Van Buynder, P., Lugg, R., Blair, P., Devine, B., Cook, A. and Weinstein, P. (2009) Indirect potable reuse: a sustainable water supply alternative. Int. J. Environ. Res. Public Health 6(3), 1174-1203.

Shah, A.D. and Mitch, W.A. (2012) Halonitroalkanes, halonitriles, haloamides, and N-nitrosamines: a critical review of nitrogenous disinfection byproduct formation pathways. Environ. Sci. Technol. 46(1), 119-131.

Sharma, V.K. and Graham, N.J.D. (2010) Oxidation of amino acids, peptides and proteins by ozone: a review. Ozone-Sci. Eng. 32(2), 81-90.

Shin, J., Hidayat, Z.R. and Lee, Y. (2015) Influence of seasonal variation of water temperature and dissolved organic matter on ozone and OH radical reaction kinetics during ozonation of a lake water. Ozone-Sci. Eng. 38(2), 100-114.

Tekle-Rottering, A., Jewell, K.S., Reisz, E., Lutze, H.V., Ternes, T.A., Schmidt, W. and Schmidt, T.C. (2016) Ozonation of piperidine, piperazine and morpholine: Kinetics, stoichiometry, product formation and mechanistic considerations. Water Res. 88, 960-971.

USGS (2014) Dissolved oxygen solubility tables. Available at: http://water.usgs.gov/software/DOTABLES/.

von Gunten, U. (2003) Ozonation of drinking water: Part I. Oxidation kinetics and product formation. Water Res. 37(7), 1443-1467.

von Gunten, U. and Hoigné, J. (1994) Bromate formation during ozonation of broide-containing waters: Interaction of ozone and hydroxyl radical reactions. Environ. Sci. Technol. 28(1234-1242).

von Sonntag, C. (2006) Free-radical-induced DNA damage and its repair: a chemical perspective. Springer-Verlag Berlin Heidelberg, Germany.

688 von Sonntag, C. and Schuchmann, H.-P. (1991) The elucidation of peroxyl radical reactions in
689 aqueous solution with help of radiation-chemical methods. Angew. Chem. Int. Ed. Engl. 30, 1229-
690 1253.
691 von Sonntag, C. and von Gunten, U. (2012) Chemistry of ozone in water and wastewater treatment -
692 from basic principles to applications. IWA Publishing, London, UK.
693 Westerhoff, P. and Mash, H. (2002) Dissolved organic nitrogen in drinking water supplies: a review.
694 J. Water Supply Res. T. 51(8), 415-448.
695 Zimmermann, S.G., Schmukat, A., Schulz, M., Benner, J., von Gunten, U. and Ternes, T.A. (2012)
696 Kinetic and mechanistic investigations of the oxidation of tramadol by ferrate and ozone. Environ.
697 Sci. Technol. 46(2), 876-884.
698
699
700

Table 1. Summary of experimental conditions

Sample	Baseline conditions	Experimental conditions
1. Nitrate and ammonium evolution during ozonation of NOM standards and real water samples		
SRHA and PLFA (IHSS)	DOC = 10 mg/L; pH = 7 (1 mM phosphate)	Specific O_3 doses: 0.4, 0.8, 1, 1.3 gO_3/gDOC
Surface water (SEQ, Australia)	DOC = 18 mg/L; O_3 = 0.75 gO_3/gDOC pH = 7 (1 mM phosphate); Inorganic carbon = 0.01 mM HCO_3^-	Specific O_3 doses = 0, 0.4, 0.75, 1 gO_3/gDOC pH = 6, 7, 8 Inorganic carbon = 0.01, 5 mM HCO_3^- t-BuOH = 10 mM; H_2O_2 = 0.4 mM
Wastewater effluent (Lausanne, Switzerland)	DOC = 6.7 mg/L (after dilution) pH = 7 (1 mM phosphate) pCBA = 1 μM	Specific O_3 doses = 0.7, 1.4, 1.9, 2.4, 2.9 gO_3/gDOC [t-BuOH (μM)]/[MeOH (μM)]= 1870/120, 1250/500, 840/750, 420/1000 Constant $^{\bullet}$OH scavenging rate = 1.4×10^6 s^{-1}
2. Nitrate yield determination from different amines		
Glycine (primary amine) Dimethylamine (secondary amine) Trimethylamine (tertiary amine)	Amine = 20 μM; O_3 = 400 μM; pH 7 (5mM phosphate); tannic acid = 3.3 μM; pCBA = 1 μM	[t-BuOH (μM)]/[MeOH (μM)]= 1870/120, 1250/500, 840/750, 420/1000 Constant $^{\bullet}$OH scavenging rate = 1.33×10^6 s^{-1}
3. Nitrate and ammonium formation using glycine		
Kinetics of NO_3^- formation from glycine	Glycine = 20 μM; O_3 = 400 μM; t-BuOH = 2.1 mM; pH 7 (10 mM phosphate)	Samples were obtained and quenched with 1 mM thiosulfate at different reaction times (until 50 min).
$^{\bullet}$OH yield determination (DMSO assay)	Glycine = 100 mM; DMSO = 10 mM; pH 7 (10 mM phosphate)	O_3 doses: 100, 175, 250, 325, 400 μM
Model DON solution (high $^{\bullet}$OH scavenging)	glycine = 20 μM; tannic acid = 3.3 μM pCBA = 0.5 μM; pH = 7 (5 mM phosphate)	Constant $^{\bullet}$OH scavenging rate = 1.3×10^6 s^{-1} [t-BuOH (μM)]/[MeOH (μM)] = 1875/125, 1460/375, 1045/625, 730/815, 417/1000; O_3 doses: 200, 300, 400 μM
Model DON solution (low $^{\bullet}$OH scavenging)	glycine = 20 μM; tannic acid = 3.3 μM pCBA = 1 μM; pH = 7 (5 mM phosphate)	Constant $^{\bullet}$OH scavenging rate = 1.8×10^5 s^{-1} [t-BuOH (μM)]/[MeOH (μM)] = 150/10, 116/30, 84/50, 59/65, 43/74 O_3 doses: 200, 250, 300, 350, 400 μM

**All experiments were performed at 22±1 ^0C*

Figure captions:

Fig. 1. NO_3^- and NH_4^+ formation during ozonation of various synthetic and natural waters at differing (a) specific O_3 doses (Suwannee River humic acid (SRHA) or Pony Lake fulvic acid (PLFA)), (b) ozonation conditions (surface water), and (c) % $^{\bullet}OH$ scavenging (wastewater effluent). Symbols in (c) are corrected NO_3^- concentrations (i.e., total measured NO_3^- (gray lines) minus predicted NO_3^- from NH_3 oxidation (Table S5)). Baseline conditions for NOM standards: DOC = 10 mg/L, DON (SRHA) = 0.26 mg/L, DON (PLFA) = 0.95 mg/L; for surface water: DOC = 18.7 ± 1.0 mg/L, DON = 0.65 ± 0.04 mg/L, specific O_3 dose = 0.75 gO_3/gDOC, pH = 7, inorganic carbon = 0.01 mM HCO_3^-, NO_3^- = 0.03 mg/L, NH_4^+ = 0.015 mg/L; for wastewater effluent: DOC = 6.7 mg/L, DON = 0.33 mg/L, pH = 7, inorganic carbon = 0.15 mM HCO_3^-, NO_3^- = 0.03 mg/L, NH_4^+ = 25.2 mg/L, $^{\bullet}OH$ scavenging rate = 1.4×10^6 s^{-1}. Error bars depict standard deviations from 3 replicate experiments.

Fig. 2. NO_3^- formation from the reactions of ozone with glycine, dimethylamine, and trimethylamine as a function of the %$^{\bullet}OH$ scavenging by t-BuOH. Conditions: amine concentration = 20 μM, tannic acid = 3 mg C/L, pH = 7, O_3 dose = 400 μM, $^{\bullet}OH$ scavenging rate = 1.33×10^6 s^{-1}, μM t-BuOH/ μM MeOH (%OH scavenging by t-BuOH) = 420/1000 (19%), 840/750 (38%), 1250/500 (57%), 1870/120 (85%). Error bars depict the mean absolute deviation (n=2).

Fig. 3. Reaction of glycine with ozone. (a) Formation of NO_3^- in excess of O_3 and complete $^{\bullet}OH$ scavenging by t-BuOH. Conditions: glycine = 20 μM, O_3 = 400 μM, pH = 7, t-BuOH = 2.1 mM, n = 2, symbols are the average experimental data and lines are from kinetic simulations (section 3.3). (b) Ammomium and $^{\bullet}OH$ concentrations for various ozone doses, correlation of NH_4^+ with $^{\bullet}OH$ formation. (c) Determination of $^{\bullet}OH$ yield by measurement of MSIA and MSOA as a function of the

ozone dose. Conditions: glycine = 100 mM, DMSO = 10 mM, pH = 7. Error bars depict standard deviations from 3 replicate experiments.

Fig. 4. NO_3^- and NH_4^+ formation from ozonation of glycine (20 μM) for varying O_3 doses and levels of $^{\bullet}OH$ scavenging. Conditions for (a-b): $^{\bullet}OH$ scavenging rate = 1.3×10^6 s^{-1}, tannic acid = 3 mg C/L, pCBA = 0.5 μM, μM t-BuOH/ μM MeOH (%OH scavenging by t-BuOH) = 417/1000 (19%), 730/815 (33%), 1045/625 (47%), 1460/375 (66%), 1875/125 (85%), pH = 7, T = 21 ± 1 ^{0}C, error bars depict standard deviations of 3 replicate experiments; (c-d): $^{\bullet}OH$ scavenging rate = 1.8×10^5 s^{-1}, tannic acid = 3 mg C/L, pCBA = 1 μM, μM t-BuOH/ μM MeOH (%OH scavenging by t-BuOH) = 43/74 (14%), 59/65 (20%), 84/50 (28%), 116/30 (39%), 150/10 (50%), pH = 7, T = 21 ± 1 ^{0}C. Symbols represent the experimental data; lines represent simulations from the model shown in Table S11 (SI).

Fig. 5. NO_3^- formation as a function of the O_3 exposure for (a-b) glycine, (c) surface water, and (d) wastewater effluent (total NO_3^- and corrected for the calculated NO_3^- formation from NH_3/NH_4^+). Conditions: (a) $^{\bullet}OH$ scavenging rate = 1.3×10^6 s^{-1}, glycine = 20 μM, tannic acid = 3 mg C/L, t-BuOH/MeOH (μM/μM) = 417/1000 – 1875/125, pH = 7; (b) $^{\bullet}OH$ scavenging rate = 1.8×10^5 s^{-1}, glycine = 20 μM, tannic acid = 3 mg C/L, t-BuOH/MeOH (μM/μM) = 43/74 – 150/10, pH 7; (c) DOC = 18.7 ± 1.0 mg/L, DON = 0.65 ± 0.04 mg/L; (d): DOC = 6.7 mg/L, DON = 0.33 mg/L, $^{\bullet}OH$ scavenging rate = 1.4×10^6 s^{-1}, t-BuOH/MeOH (μM/μM) = 420/1000 – 1870/120.

Fig. 6. Proposed mechanism for the ozone-glycine reaction system: nitrate and ammonium formation

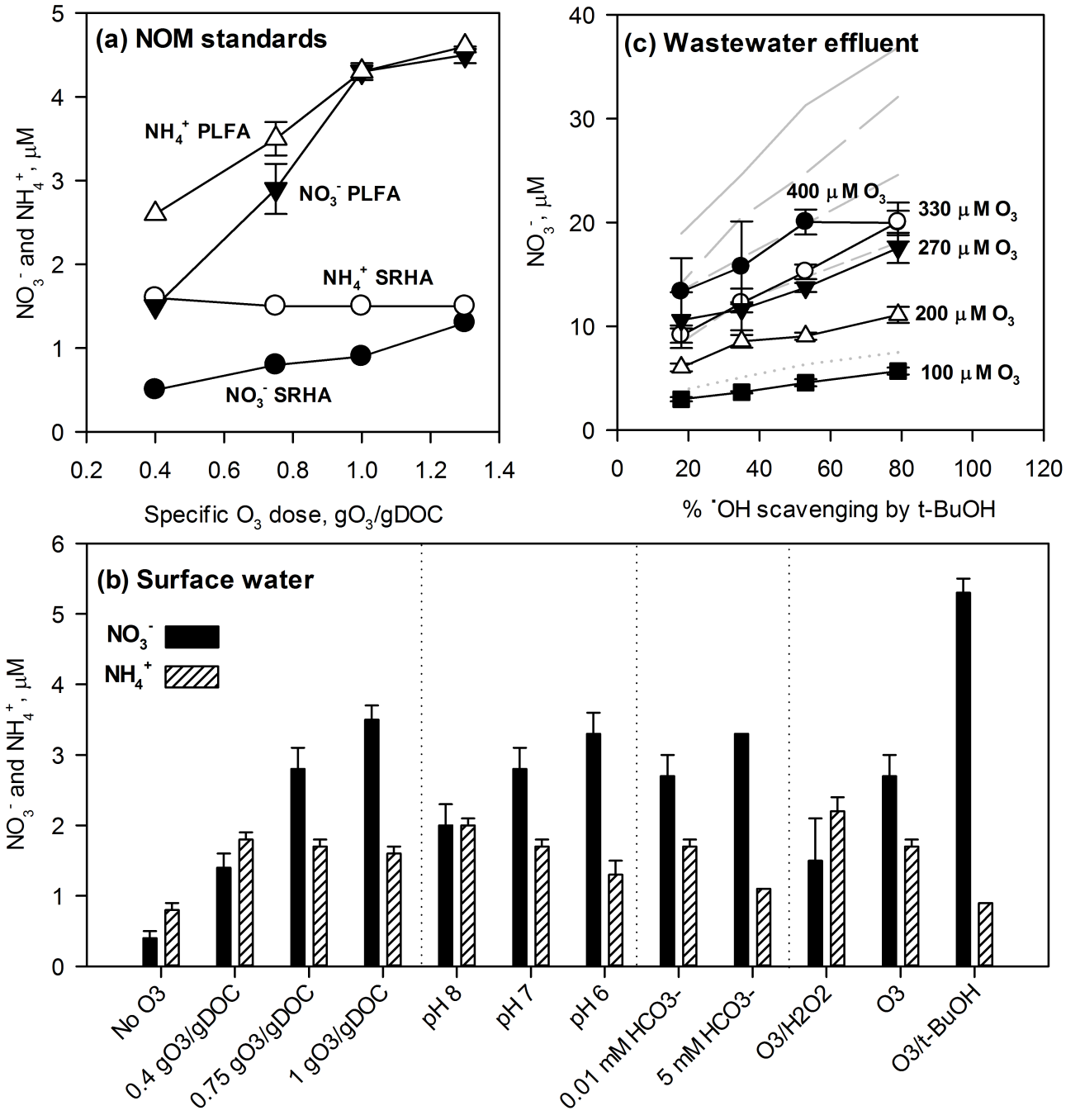
(a) NOM standards
NH4+ PLFA
NO3- PLFA
NH4+ SRHA
NO3- SRHA
NO3- and NH4+, μM
Specific O3 dose, gO3/gDOC
(c) Wastewater effluent
400 μM O3
330 μM O3
270 μM O3
200 μM O3
100 μM O3
NO3-, μM
% •OH scavenging by t-BuOH
(b) Surface water
NO3-
NH4+
NO3- and NH4+, μM
No O3
0.4 gO3/gDOC
0.75 gO3/gDOC
1 gO3/gDOC
pH 8
pH 7
pH 6
0.01 mM HCO3-
5 mM HCO3-
O3/H2O2
O3
O3/t-BuOH

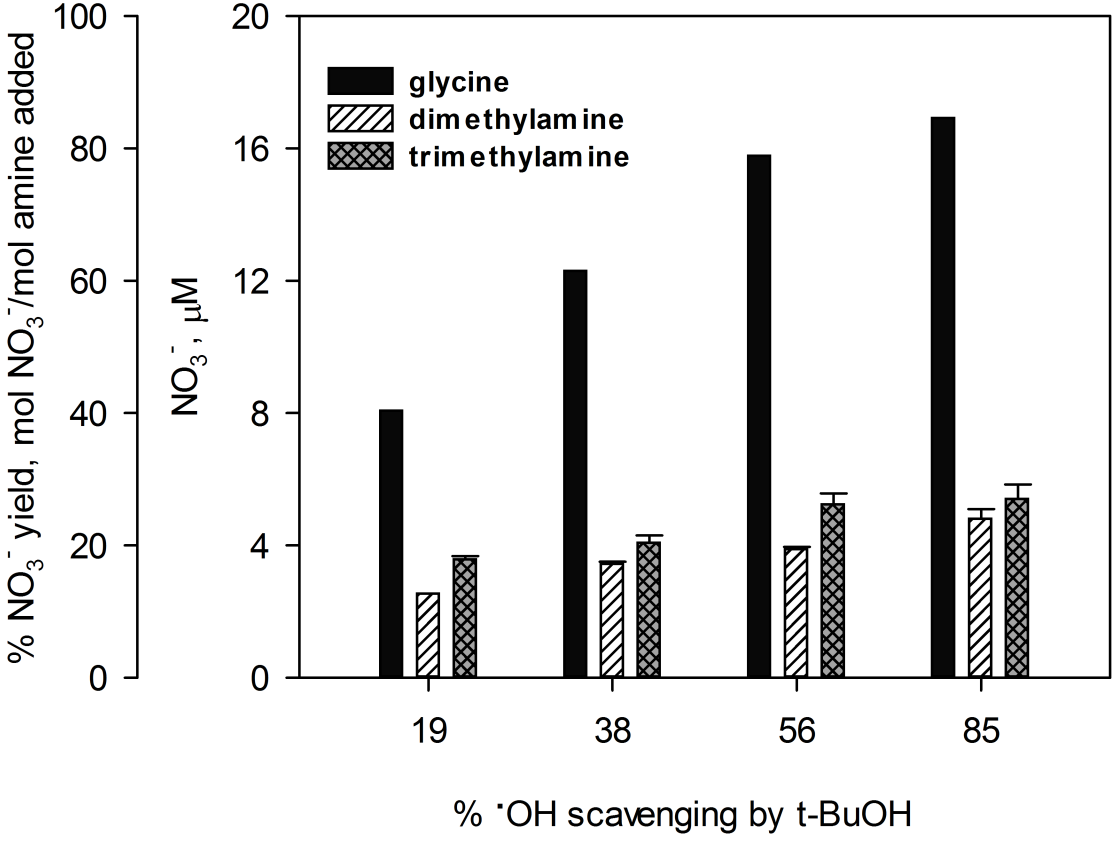
% NO_3^- yield, mol NO_3^-/mol amine added
NO_3^-, µM
glycine
dimethylamine
trimethylamine
100
80
60
40
20
0
20
16
12
8
4
0
19
38
56
85
% •OH scavenging by t-BuOH

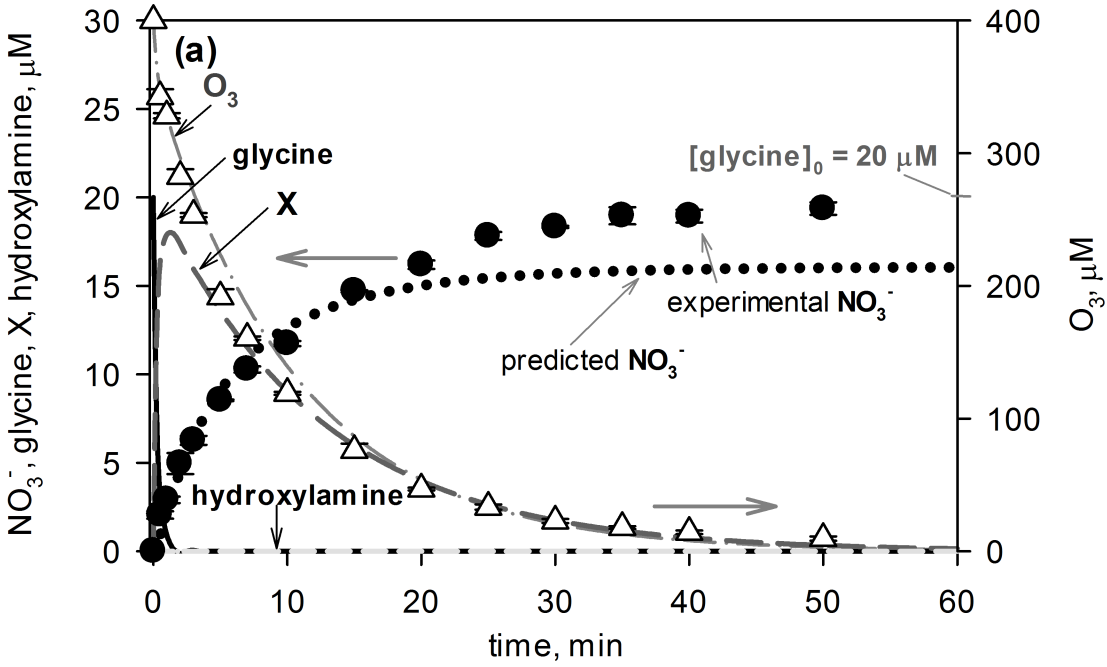
(a)
O_3
glycine
X
hydroxylamine
[glycine]$_0$ = 20 μM
experimental NO_3^-
predicted NO_3^-
NO_3^-, glycine, X, hydroxylamine, μM
O_3, μM
time, min

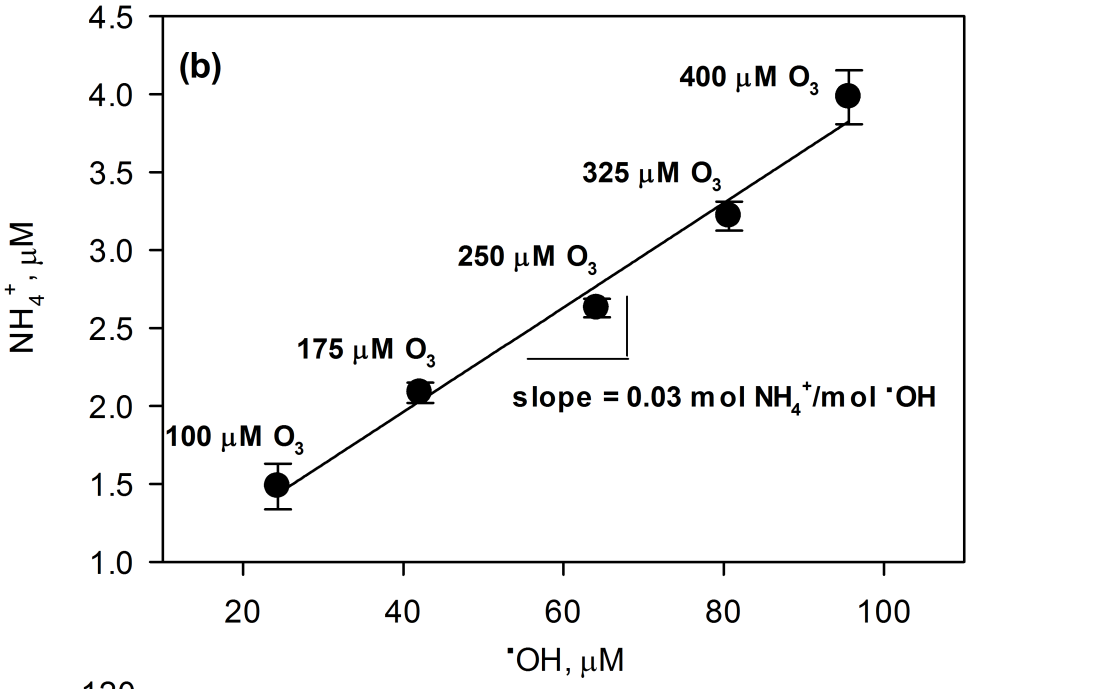
(b)
400 μM O_3
325 μM O_3
250 μM O_3
175 μM O_3
100 μM O_3
slope = 0.03 mol NH_4^+/mol •OH
NH_4^+, μM
•OH, μM

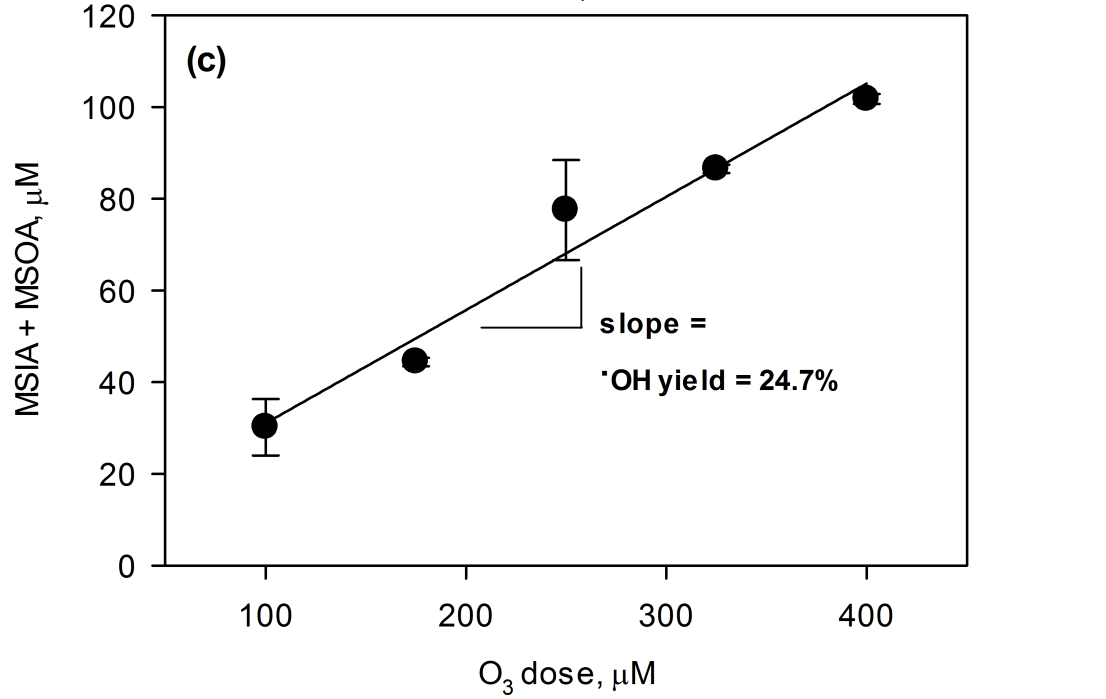
(c)
slope =
•OH yield = 24.7%
MSIA + MSOA, μM
O_3 dose, μM

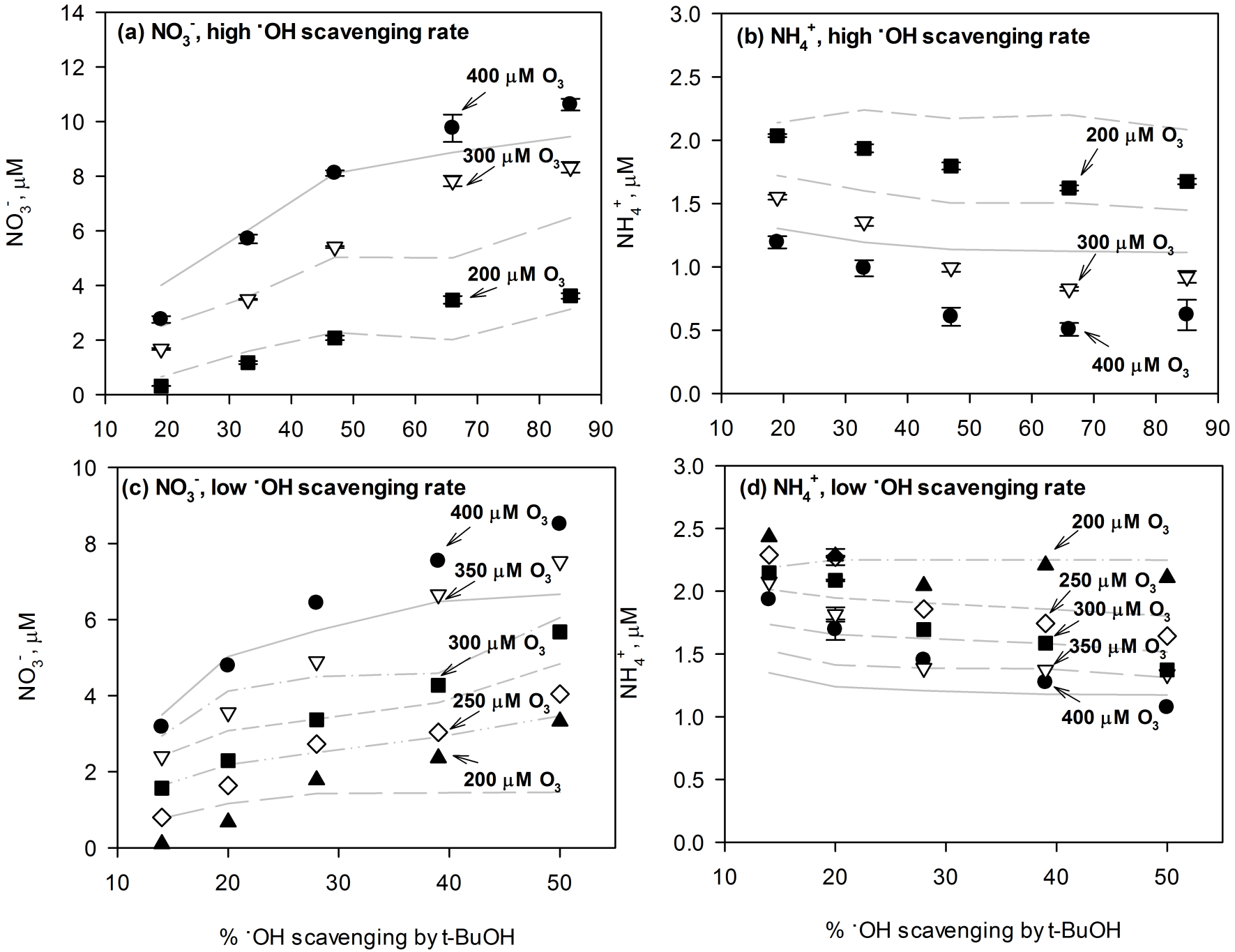
(a) NO3-, high ·OH scavenging rate
400 μM O3
300 μM O3
200 μM O3
NO3-, μM
(b) NH4+, high ·OH scavenging rate
200 μM O3
300 μM O3
400 μM O3
NH4+, μM
(c) NO3-, low ·OH scavenging rate
400 μM O3
350 μM O3
300 μM O3
250 μM O3
200 μM O3
NO3-, μM
% ·OH scavenging by t-BuOH
(d) NH4+, low ·OH scavenging rate
200 μM O3
250 μM O3
300 μM O3
350 μM O3
400 μM O3
NH4+, μM
% ·OH scavenging by t-BuOH

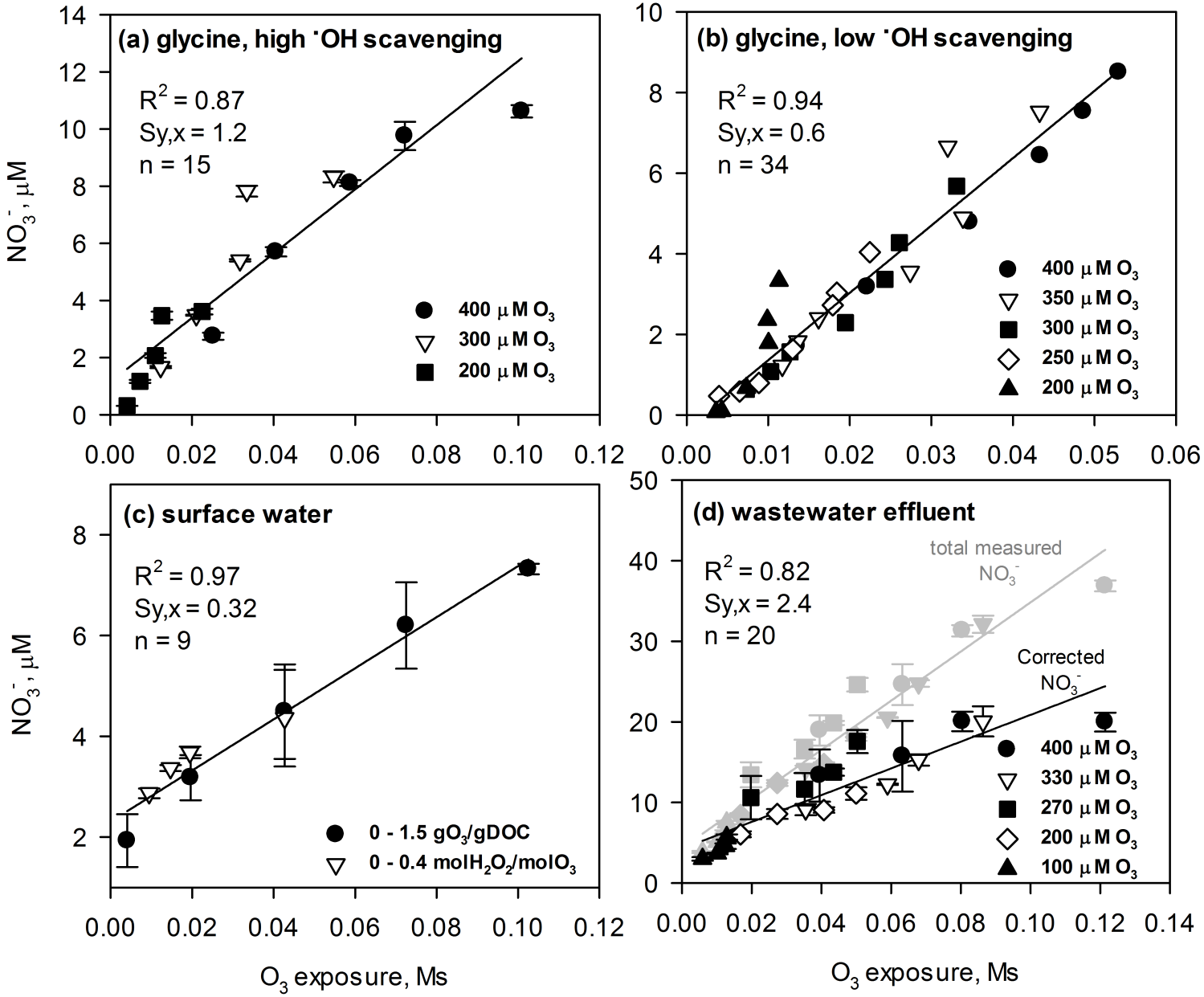
(a) glycine, high ·OH scavenging
R2 = 0.87
Sy,x = 1.2
n = 15
400 µM O3
300 µM O3
200 µM O3
(b) glycine, low ·OH scavenging
R2 = 0.94
Sy,x = 0.6
n = 34
400 µM O3
350 µM O3
300 µM O3
250 µM O3
200 µM O3
(c) surface water
R2 = 0.97
Sy,x = 0.32
n = 9
0 - 1.5 gO3/gDOC
0 - 0.4 molH2O2/molO3
(d) wastewater effluent
R2 = 0.82
Sy,x = 2.4
n = 20
total measured NO3-
Corrected NO3-
400 µM O3
330 µM O3
270 µM O3
200 µM O3
100 µM O3
NO3-, µM
O3 exposure, Ms

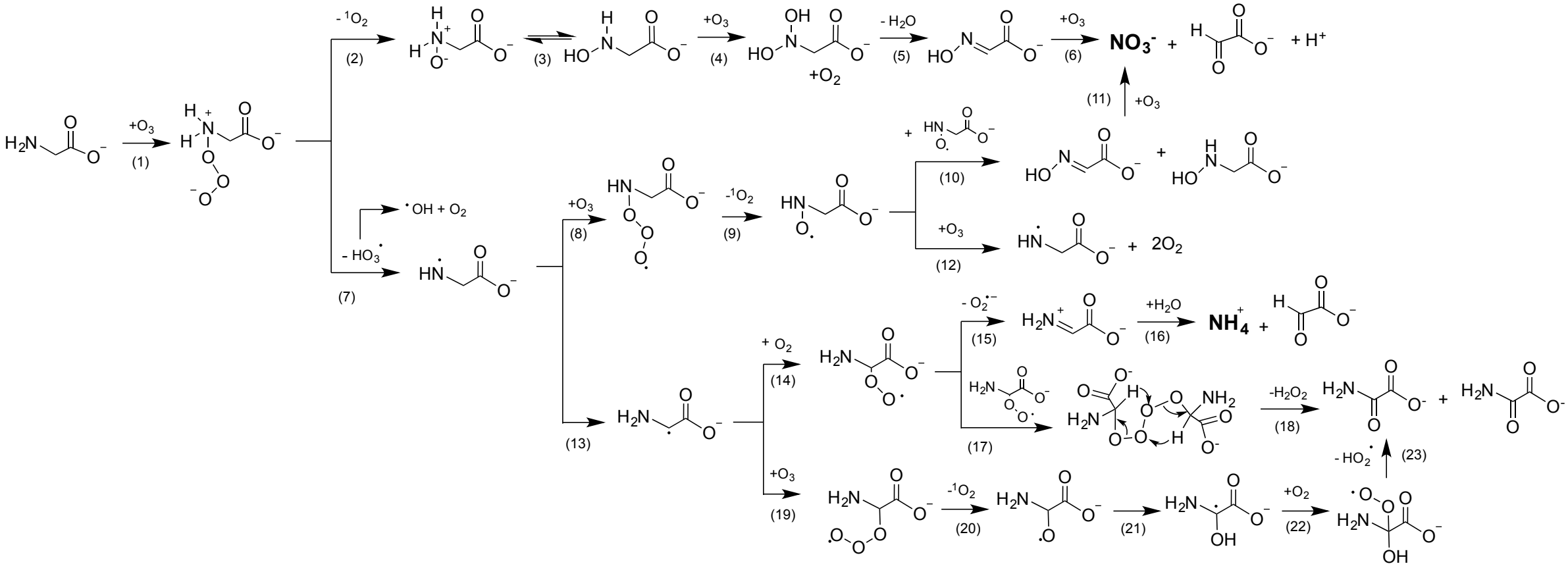
+O3
(1)
- 1O2
(2)
(3)
+O3
(4)
+O2
- H2O
(5)
+O3
(6)
NO3-
+ H+
(11)
+O3
- HO3•
•OH + O2
(7)
+O3
(8)
-1O2
(9)
+
(10)
+O3
(12)
+ 2O2
+ O2
(14)
(13)
+O3
(19)
- O2•−
(15)
+H2O
(16)
NH4+
(17)
-H2O2
(18)
-1O2
(20)
(21)
+O2
(22)
- HO2•
(23)

Highlights:

- Ozonation of dissolved organic nitrogen forms NO_3^- and NH_4^+
- NO_3^- concentrations correlate with O_3 exposures
- Lower O_3 doses cause higher NH_4^+ concentrations
- Amine-N oxidation from oxygen transfer induces NO_3^- formation
- NH_4^+ is induced from electron-transfer reaction involving ozone